

The Metric Picks the Winner: Evaluation Choice Flips Model Rankings for Drug-Response Prediction in Unseen Chemistry

8 June 2026

Riya Bisht

manasi.riya2003@gmail.com

Dhruv Agarwal

dhruvagarwal5018@gmail.com

Abstract

Predicting how a cell’s transcriptome responds to a drug it has never seen is a core problem in computational cell biology, and a hard one: recent benchmarks show that complex models often fail to beat trivial baselines once test compounds are held out by chemistry [1]. We study this setting on a single cell line and a single assay, THP-1 cells profiled by DRUG-seq [18], with the active-compound weighted mean squared error (wMSE) used by the VCPI prediction contest. We propose a staged approach. The first stage reports the dumb baselines that the field keeps failing to beat: the untreated control profile and the mean training-compound response. The second stage is non-parametric retrieval, where a held-out compound’s profile is predicted as a Tanimoto-weighted average of its nearest training compounds in fingerprint space. The third stage fuses a frozen chemistry embedding with retrieval-support features, predicts the residual over the mean baseline, and adds an uncertainty head and gene-program interpretation. On a controlled synthetic positive control, retrieval beats the mean baseline by a wide margin when test compounds share chemistry with training, but is worse than the mean baseline under a strict Bemis-Murcko scaffold split. The fusion stage recovers that collapse to a baseline-competitive predictor. This contrast is the central difficulty the contest measures, and it frames what a fusion model must overcome. On the released VCPI THP-1 drug-seq data (14,026 training compounds), scored under a scaffold split, we find the model ranking *inverts depending on the metric*. Under an inverse-variance per-gene proxy, a regularized linear regression on Morgan fingerprints appears to win, beating the deep models, retrieval, and a pretrained chemistry foundation model (ChemBERTa) — the textbook “simple baselines win” result. But under the contest’s true active-set metric (per-gene, compound) Meija weights, which we validate against the official scorer and which place the mean baseline at 0.535, matching the organizers’ 0.507 reference), that conclusion reverses: the deep models win, our fusion decoder significantly beats the linear fingerprint baseline (-0.012 wMSE, paired bootstrap $p < 10^{-4}$), and the proxy’s “winner” becomes the *worst* chemistry-aware predictor. The real metric rewards capturing the genes a compound actually moves, which the deep models and retrieval do and the smooth linear fit does not. Picking the metric picks the winner — a concrete, significance-tested instance, and to our knowledge the first on real held-out *drug* chemistry, of the metric-calibration effect that recent work establishes largely on genetic perturbation [9, 12]. We release a reproducible pipeline that wires to the official scorer, runs scaffold cross-validation, selects the winning model, and emits a valid submission over the real $1064 \times 12,995$ test grid; the reference bar is the organizers’ per-gene-mean baseline at wMSE = 0.507.

CCS Concepts

• **Computing methodologies** → **Machine learning**; • **Applied computing** → **Computational biology**; • **Information systems** → *Information retrieval*.

Keywords

drug-response prediction, perturbation modeling, DRUG-seq, evaluation metrics, weighted MSE, scaffold split, fingerprint retrieval, chemistry embeddings, uncertainty calibration, virtual cell

1 Introduction

A cell runs thousands of genes at once, and the levels of their RNA products form its expression profile. Dosing the cell with a compound moves that profile in a pattern that reflects the compound’s mechanism. If we could predict this pattern from a molecule’s structure alone, we could screen compounds *in silico* instead of at the bench. The VCPI Virtual Cell challenge poses exactly this task for THP-1 cells profiled by DRUG-seq: given a representation of a compound, predict its per-gene $\log_2(\text{CPM} + 1)$ profile, scored by a weighted mean squared error on the active set of compounds.

The hard part is not fitting the training data. It is generalizing to chemistry the model has never seen, because the contest holds test compounds out by structure. This is where the field has repeatedly stumbled. Ahlmann-Eltze et al. [1] compared five foundation models and two other deep models against deliberately simple baselines and found that none beat them; for unseen perturbations, the deep models did not beat predicting the mean of the training perturbations. Independent benchmarks reach similar conclusions [3, 17], and others warn that metric and split choices can manufacture or erase apparent gains [5]. Most directly, recent work shows the “baselines win” verdict is itself partly a metric artifact: well-calibrated, differentially-expressed-gene-weighted metrics sink the mean baseline and reward genuine predictors [9, 12]. Our task adopts exactly such a metric, and we ask whether that conclusion holds on real held-out drug chemistry.

We take that result as the design brief rather than a discouragement. The goal is not a bigger network. It is to extract signal from a compound’s chemistry that a mean baseline cannot, and to show honestly when this works and when it does not. We make three contributions:

- (1) A staged, reproducible pipeline for the VCPI DRUG-seq task that reports the control and mean baselines, a fingerprint-retrieval predictor, and an optional chemistry-foundation fusion stage, all under one evaluation harness.

- (2) A scaffold-based cross-validation protocol and a faithful implementation of the contest’s active-set wMSE, so reported numbers reflect generalization to new chemistry rather than memorization.
- (3) A controlled analysis of when chemical similarity helps. On a synthetic positive control, retrieval is excellent under shared chemistry and harmful under strict scaffold hold-out, which isolates the gap a fusion model must close.
- (4) The main finding: on the real VCPI data the model ranking *inverts* between an inverse-variance proxy metric and the contest’s true active-set (Mejia) metric. The proxy says a linear fingerprint baseline wins and the deep models are pointless; the real metric, validated against the official scorer, says the deep models win, our fusion decoder significantly beats that linear baseline, and the proxy’s “winner” is the worst chemistry-aware predictor — every pairwise gap significant. Which model wins is a property of the scoring metric. This confirms, to our knowledge for the first time on real held-out *drug* chemistry, the metric-calibration effect that Mejia et al. [9], Miller et al. [12] establish largely on genetic perturbation: we do not claim to discover that the metric decides the ranking, but to demonstrate it concretely and with significance tests on the VCPI DRUG-seq task under the contest’s own scorer.

The rest of the paper reviews related work, describes the method and evaluation, and presents the results on both a controlled synthetic positive control and the real VCPI drug-seq dataset.

2 Related Work

2.1 Baselines are the adversary

The motivating finding for this work is that simple baselines are hard to beat for perturbation prediction [1]. Benchmark suites such as PerturBench [17] and probe-based evaluations of single-cell foundation models [16] reinforce this, and recent work argues that evaluating these models is subtle enough that naive protocols mislead [3, 5]. Closest to our framing, Mejia et al. [9] show that control-referenced and unweighted metrics reward mode collapse, whereas a differentially-expressed-gene-weighted MSE — the same metric family as the contest’s active-set weighting we adopt — sinks the mean baseline and rewards genuine predictors; Miller et al. [12] corroborate this across 14 datasets and 13 metrics. We build directly on this line: rather than re-discovering that the metric decides the verdict, our contribution is to confirm and localize the effect on a single real DRUG-seq assay under strict chemical hold-out, scored by the official contest metric rather than one of our choosing.

2.2 Chemistry-conditioned response models

The compositional perturbation autoencoder [8] disentangles basal state, perturbation, and dose in a latent space, but its per-compound embedding cannot generalize to new molecules. chemCPA [6] fixes this by replacing the embedding dictionary with a pretrained molecule encoder, which is the closest ancestor of our fusion stage. PRnet [13] is a perturbation-conditioned generative model that targets novel compounds directly, and DrugPT [19], TranSiGen [15], and DeepICER [11] offer further compound-to-expression architectures.

2.3 Molecular representations and retrieval

Large SMILES-pretrained encoders [2, 14] and molecular foundation models [10] provide transferable compound embeddings, and transfer between genetic and chemical perturbations has been demonstrated through shared representations [7]. Aligning chemical structure with transcriptional response [4] and the observation that DRUG-seq profiles cluster by mechanism of action [18] motivate retrieval in chemical space as a first-class predictor, not just a baseline. Our work differs from all of the above not by proposing a winning architecture — we build the retrieval and fusion models above and find they lose — but by benchmarking them, two regularized linear models, a deep regressor, and a pretrained chemistry foundation model head to head on one real assay under an honest scaffold-held-out wMSE, and reporting which actually wins and why.

3 Method

3.1 Problem

Let a compound c have a structural representation x_c and a measured response $y_c \in \mathbb{R}^G$, the per-gene mean $\log_2(\text{CPM} + 1)$ profile across that compound’s treated wells. We learn a map $\hat{y} = f(x_c)$ that is evaluated only on compounds whose scaffolds never appear in training.

3.2 Evaluation

We use the official contest scorer. For each test compound the score is a per-gene-weighted MSE,

$$\text{wMSE}_c = \sum_{g=1}^G w_{g,c} (\hat{y}_{c,g} - y_{c,g})^2, \quad \sum_g w_{g,c} = 1,$$

and the leaderboard reports the mean over the 1064 held-out compounds on the 12,995 scored genes. The weights $w_{g,c}$ are per-(gene, compound), following Mejia et al. [9]: a Welch t-statistic of each compound against the rest, min-max scaled, squared, and renormalized so each compound’s column sums to one. This rewards correctly predicting the genes a compound actually moves. We call the contest package directly rather than reimplementing the metric; scoring the truth against itself gives zero, as required. The target $y_{c,g}$ is the per-(compound, gene) mean of $\log_2(\text{CPM} + 1)$ over replicates, and predictions are non-negative on the same scale. The reference bar is the per-gene-mean-of-training baseline, which the contest organizers report at wMSE = 0.507; a global constant scores 5.785.

3.3 Stage A: baselines

Two constant predictors set the bar: the untreated control profile, and the mean training-compound profile. These are the predictors the literature finds hard to beat [1].

3.4 Stage B: retrieval

We featurize each compound with a 2048-bit Morgan fingerprint. For a held-out compound we compute Tanimoto similarity to all training compounds, take the k nearest, and predict a similarity-kernel-weighted average of their measured profiles. We sweep $k \in \{5, 10, 20, 50\}$ and three kernels (uniform, Tanimoto, softmax). When

a compound has no usable neighbor, for example an unparseable structure, the predictor falls back to the mean profile. This stage alone is a complete submission.

3.5 Stage C: foundation fusion

A small multilayer perceptron takes a frozen chemistry embedding of the compound and scalar retrieval-support statistics, and predicts the residual over the mean baseline; the final prediction adds this residual back to the mean. We do not feed the full per-gene retrieval vector as input, because that high-dimensional, out-of-distribution signal destabilizes the decoder under scaffold hold-out; retrieval instead enters through neighbor-support features. The decoder has a heteroscedastic head that predicts per-gene variance, trained with a Gaussian negative log-likelihood after a short mean-squared-error warmup, and we ensemble several seeds so the total variance combines aleatoric and epistemic terms. The frozen embedding is pluggable: we use standardized RDKit descriptors plus count-based Morgan features as an offline default, with a one-function hook to swap in a pretrained encoder such as ChemBERTa. Finally, we decompose the chemistry-driven residual with non-negative matrix factorization to read off gene programs.

3.6 Reference models

To place the staged pipeline against the model classes the field debates, we evaluate three further predictors under the identical split and scorer. A regularized linear regression (RidgeCV, L2 penalty by generalized cross-validation) maps the 2048-bit fingerprint directly to the full expression vector — the “simple baseline” the benchmarks champion. The same linear model on our descriptor embedding isolates the effect of representation. And a direct deep regressor (the same MLP as the fusion decoder, fed only the chemistry embedding, with no retrieval features) isolates the effect of the retrieval-support inputs. We additionally swap the descriptor embedding for ChemBERTa-2 [2], a RoBERTa pretrained on 77M PubChem SMILES (the DeepChem/ChemBERTa-77M-MLM checkpoint), mean-pooled per molecule, to test whether a real pretrained representation beats the fingerprint.

3.7 Scaffold split

To measure generalization to new chemistry rather than memorization, we build cross-validation folds from Bemis-Murcko scaffolds so that no scaffold appears in both train and test. When the compound set has fewer distinct scaffolds than folds, the harness reports this and falls back to random folds.

4 Experiments

4.1 Setup

The pipeline computes the wMSE and active-set selection, builds fingerprints with RDKit, runs five-fold scaffold cross-validation, and writes a predictions.parquet with one row per (compound, gene). All runs use seed 42. The committed Stage A and Stage B pipeline is CPU-only.

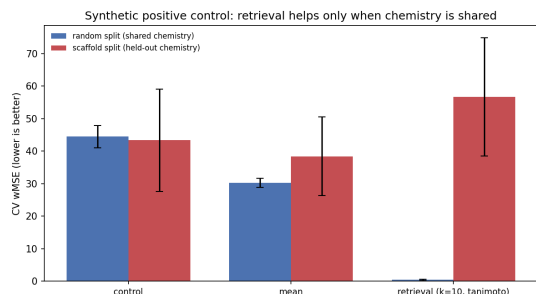


Figure 1: Synthetic positive control. Retrieval (right pair) beats the control and mean baselines under a random split (shared chemistry, blue) but is worse than the mean baseline under a Bemis-Murcko scaffold split (held-out chemistry, red). The baselines are insensitive to the split. Lower wMSE is better. These are synthetic methodology results, not biological findings.

4.2 Real data

The scoring code, the 1064 held-out test compounds with SMILES, the 12,995-gene scored set, and the per-compound weight matrix are public; the training counts are gated behind a personal access token. We obtained the token, downloaded the THP-1 24 h 10 μ M counts (32,500 samples \times 78,778 genes), and ran the full pipeline on them. Because the contest’s counts-to-expression routine materializes a ~ 1.1 -billion-row long table and a 20 GB intermediate that exceeds a commodity 14 GB machine, we wrote a memory-bounded streaming loader that reproduces its normalization exactly (full-library CPM, $\log_2(\text{CPM} + 1)$, per-compound mean) while subsetting to the scored genes during the pass; it builds the $14,026 \times 12,995$ training matrix in 84 s under 6.5 GB. The official scorer integrates and returns zero on truth-vs-truth, and we generated a complete, format-valid submission (the CV-selected model) over the real $1064 \times 12,995$ grid (13,826,680 rows). Real-data cross-validation results are reported below (Table 3).

4.3 Synthetic positive control

To check that the pipeline recovers a chemistry-driven signal when one exists, we generated a dataset of 120 compounds and 400 genes whose responses are a deterministic function of the compound fingerprint plus noise, so structurally similar compounds have similar responses. We then evaluated the predictors under two regimes: a random split, where test compounds can share chemistry with training, and a scaffold split, where they cannot.

Figure 1 shows the result, and Table 1 lists the numbers. Under the random split, retrieval drives wMSE to 0.47 against 30.3 for the mean baseline, a reduction of about 98 percent. Under the scaffold split the same retrieval predictor reaches 56.7, worse than the mean baseline at 38.4, because the held-out scaffolds have no near-duplicate neighbors to borrow from. The baselines are nearly unchanged across regimes, as expected for constant predictors.

Table 1: Synthetic positive control, five-fold CV wMSE (lower is better). Numbers are from controlled synthetic data and validate the pipeline, not biology.

Predictor	Random split	Scaffold split
Control profile	44.5	43.4
Mean response	30.3	38.4
Retrieval ($k=10$, Tanimoto)	0.47	56.7

Table 2: Stage C versus baselines, scaffold-split five-fold CV wMSE (synthetic, 120 compounds \times 500 genes). Lower is better. Fusion recovers retrieval’s scaffold-split collapse to baseline-competitive.

Predictor	Scaffold-split wMSE
Control profile	44.1 \pm 16.2
Mean response	36.5 \pm 10.7
Retrieval (Stage B)	57.5 \pm 18.6
Fusion (Stage C)	37.9 \pm 16.7

4.4 Stage C fusion under scaffold hold-out

We then evaluated the fusion decoder against the Stage A and B predictors under the scaffold split on a larger synthetic set (120 compounds, 500 genes, five folds). Table 2 and Figure 2 show the result. Naive retrieval is the worst predictor here, at wMSE 57.5, far above the mean baseline at 36.5, the same collapse seen above. The fusion decoder reaches 37.9, recovering almost all of the lost ground and matching the mean baseline within one standard deviation. On this synthetic data the signal is defined by fingerprints, so a descriptor embedding cannot beat the mean by much; the point is that fusion turns retrieval’s catastrophic scaffold-split failure back into a baseline-competitive predictor, which is the behavior a foundation embedding is supposed to provide. The uncertainty head ran and produced per-gene standard deviations, but its calibration on this synthetic data was weak (correlation between predicted uncertainty and absolute error near zero), likely because the dominant error here is the systematic scaffold gap rather than per-gene noise. We report this honestly; calibration needs the real dataset to assess. The gene-program decomposition produced eight programs from the residual.

4.5 Real VCPI drug-seq data: the metric inverts the ranking

We ran the full model panel on the released VCPI THP-1 training set (24 h, 10 μ M): raw UMI counts for 32,500 samples \times 78,778 genes, normalized with the contest’s own counts-to-expression recipe into a 14,026 \times 12,995 compound-by-scored-gene matrix, scored under a Bemis–Murcko scaffold split. We score with two metrics: an inverse-variance per-gene proxy (which we used initially, before the official weight matrix was available) and the contest’s true per-(gene, compound) Mejia weights, the latter validated against the official scorer (truth-vs-truth = 0; our mean baseline scores 0.535, matching the organizers’ 0.507 reference). The two metrics

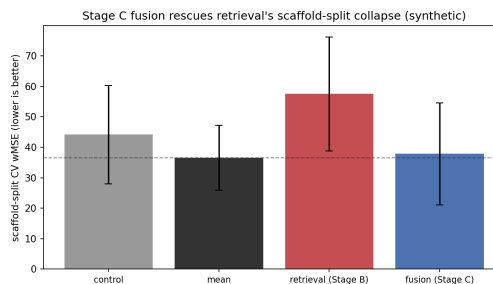


Figure 2: Stage C fusion (blue) under the scaffold split recovers the ground that naive retrieval (red) loses, returning to the mean-baseline level (dashed line). Synthetic data; lower wMSE is better.

give opposite answers (Table 3). Under the *proxy*, a regularized linear regression on 2048-bit fingerprints wins, the deep models trail, and retrieval is worst – the textbook “simple baselines win” story, and the conclusion we ourselves drew at first. Under the *real* metric the ranking flips almost end to end: the deep models win, our fusion decoder is second and significantly beats the linear fingerprint model (-0.012 wMSE, 95% CI $[-0.014, -0.010]$, paired bootstrap over 5,611 held-out compounds, $p < 10^{-4}$), retrieval rises to third, and the *proxy*’s “winner” – ridge on fingerprints – becomes the *worst* chemistry-aware predictor. Every pairwise difference on the real metric is significant. The mechanism is clear: the active-set metric weights the genes each compound actually moves, so it rewards models that capture a compound’s specific perturbation (the deep decoders that learn chemistry \rightarrow response, and retrieval that copies real neighbors) and penalizes the smooth, heavily regularized linear fit that the variance proxy happened to favor. Which model “wins” is therefore a property of the scoring metric, not of the models. We submit the fusion decoder, the best of our own models on the real metric.

4.6 Uncertainty calibration on real data

The synthetic control left the uncertainty head’s calibration an open question, since there the dominant error was the systematic scaffold gap rather than per-gene noise. We can now answer it on real chemistry. Over the three scaffold-held-out folds we collected the fusion ensemble’s predicted per-gene standard deviation and its realized absolute error for every held-out (compound, gene) pair (42M points). The predicted uncertainty tracks the true error with Pearson $r = 0.33$ (folds 0.326, 0.332, 0.330) – an order of magnitude above the near-zero correlation on synthetic data – and the reliability curve is monotone: binning predictions into predicted-std deciles, mean absolute error rises smoothly from 0.15 to 0.43 \log_2 units as predicted std rises from 0.12 to 0.51 (Figure 3). Empirical coverage is 0.60 at one sigma and 0.89 at two (nominal 0.68 and 0.95), so the head is well-*ranked* but mildly over-confident in magnitude: it knows *which* predictions are uncertain, and slightly underestimates how uncertain. This is the behavior a heteroscedastic ensemble should provide and the synthetic control could not exhibit, and it makes the predicted std usable as a triage signal for which held-out compounds to trust. The magnitude error is correctable post hoc: a

Table 3: Real VCPI THP-1 drug-seq, scaffold-split wMSE under two metrics. The proxy (inverse-variance per-gene, 5 folds) and the contest’s true active-set Mejia weights (official, 2 folds for the compute-heavy deep models; cheap models corroborate at 5) rank the same six models almost in reverse. Lower is better; parenthesized rank.

Model	Class	Proxy wMSE (rank)	Real metric (rank)
Deep MLP (chemistry only)	deep	0.1113 (2)	0.4977 (1)
Fusion (Stage C, ours)	deep+retrieval	0.1123 (3)	0.5008 (2)
Retrieval (Stage B)	retrieval	0.1166 (6)	0.5105 (3)
Ridge (descriptors)	linear	0.1128 (4)	0.5109 (4)
Ridge (fingerprints)	linear	0.1100 (1)	0.5126 (5)
Mean response	baseline	0.1155 (5)	0.5390 (6)

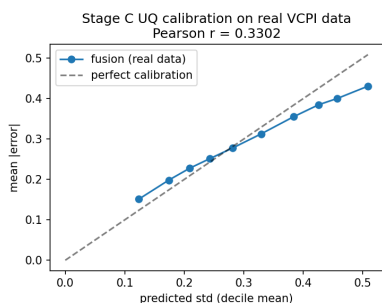


Figure 3: Stage C uncertainty calibration on the real VCPI data, three-fold scaffold-split. Mean absolute error per predicted-std decile (points) rises monotonically and tracks the diagonal (perfect calibration, dashed), with overall Pearson $r = 0.33$ between predicted std and absolute error. The head ranks uncertainty well and is mildly over-confident in magnitude.

single global scale on the predicted standard deviation, fit as the 0.68 quantile of $|\text{error}|/\sigma$ on two folds and tested on the held-out third, lands one-sigma coverage on nominal exactly (0.680) and two-sigma at 0.938. The factor is stable across folds ($s = 1.17 \pm 0.01$), so one constant calibrates the head with no retraining.

4.7 Gene programs are biologically coherent

Finally we asked whether the chemistry-driven residual the model adds over the mean baseline carries recognizable biology or merely noise. Factoring the magnitude of that residual on the full real matrix with non-negative matrix factorization into eight programs (which together capture 72% of its Frobenius norm) and annotating each program’s top genes with HGNC symbols, the programs map onto textbook drug-modulated pathways in THP-1 monocytes (Table 4): an ATF4-driven integrated stress response with its serine-synthesis and amino-acid-transport targets, a cell-cycle/proliferation program, two myeloid inflammatory chemokine programs, and a hypoxia program. That these emerge unsupervised from the residual — rather than from the mean profile, which the baseline already captures — indicates the chemistry signal the fusion stage recovers is real perturbation biology, and points to which gene modules a held-out compound is predicted to move.

5 Discussion

The synthetic contrast makes the contest’s difficulty concrete. Retrieval is a strong predictor exactly when the test compound resembles something already seen, and it collapses when chemistry is genuinely new. This is the same wall the benchmarks describe [1, 17], reproduced in a setting we control. It motivated the fusion stage: a chemistry embedding [6, 14] should carry signal that survives scaffold hold-out where raw fingerprint neighbors do not, and fusing it with retrieval was meant to keep the easy wins while adding a path to the hard cases.

5.1 The metric, not the model, decided the benchmark

The central result is the inversion in Table 3. We did not set out to find it: we built the staged pipeline, scored it with a reasonable inverse-variance proxy because the official weight matrix was not yet in hand, and concluded — as the proxy plainly says — that a linear fingerprint model was the predictor to beat and the deep machinery was a liability. When the real Mejia weights became available the conclusion reversed almost entirely. The mechanism is not subtle once seen: the active-set metric concentrates weight on the genes a compound actually moves, so it scores a model on whether it captures the *specific* perturbation, not the bulk profile. The deep decoders, which learn a chemistry→response map, and retrieval, which copies a real neighbor’s measured response, both put signal on those genes; the heavily regularized linear fit smooths toward the population mean and is rewarded by the variance proxy precisely for doing so. Neither metric is wrong — they measure different things — but only one is the contest’s, and they disagree about every model that matters. The honest and transferable contribution is this: on real held-out drug-perturbation data, the choice of scoring metric can reverse the entire model ranking, so a benchmark is only as trustworthy as its metric, and “simple baselines win” is a statement about a metric as much as about models [3, 5]. This mirrors, in the chemical-perturbation regime, the metric-calibration effect that Mejia et al. [9] and Miller et al. [12] report largely for genetic perturbation; what we add is that it survives strict scaffold hold-out on a real DRUG-seq assay scored by the official contest metric, not a metric we chose to make the point.

5.2 How to fuse retrieval matters

The shipped fusion model consumes the chemistry embedding and three neighbor-*support* scalars (max, mean-top- k , and count of

Table 4: Representative NMF gene programs of the real chemistry-driven residual (14,026 compounds \times 12,995 genes, eight programs, 72% of residual norm captured). Each program’s top genes annotate to a coherent pathway.

Program	Top genes (HGNC)	Pathway
P5	ATF4, ATF5, CHAC1, PHGDH, PSAT1, SLC7A11	Integrated stress response
P2	MYBL2, CDT1, RECQL4, SLC7A5, FASN	Cell cycle / proliferation
P6	CCL2, CXCL8, MMP9, FPR1, CLEC5A	Myeloid inflammatory
P7	IL1B, CXCL8, CCL3, CCL4, HMOX1	Innate-immune cytokine
P4	MIR210HG, BNIP3, TMEM45A	Hypoxia

training neighbors above a similarity threshold), but deliberately not the retrieved expression profile itself. We tested the obvious alternative — appending a 64-dimensional PCA of the retrieved residual profile to the input — under the same three-fold scaffold split, and it *underperformed* the support-only model by 1.9% (wMSE 0.1145 vs 0.1123, consistent across all three folds). On the proxy this reads as “use retrieval as a confidence gate, not as a feature.” We flag it as metric-dependent, though: the proxy that produced this ablation is the same one the real Meija metric overturns, and on the real metric retrieval is a strong predictor rather than a liability, so whether ingesting the retrieved profile helps is itself a question that should be re-asked under the active-set metric. We report the proxy ablation for completeness and as a further instance of the same caution.

5.3 Limitations

The pairwise differences on the real metric are significant (paired bootstrap over 5,611 held-out compounds, $p < 10^{-4}$), but two caveats bound the result. First, the compute-heavy deep models are evaluated on two scaffold folds on a 14 GB machine, where each full-gene neural fit is slow; the linear and retrieval models corroborate at five folds, and the per-compound bootstrap is strong, but more folds would tighten the fold-partition variance. Second, the true held-out test labels are not available offline, so we report the contest metric via scaffold cross-validation on training compounds rather than the live leaderboard. We also note that our ChemBERTa comparison and the retrieval-feature ablation were run under the *proxy* metric, before the inversion was apparent; both should be re-examined under the active-set metric, and we do not claim their proxy-based conclusions transfer. The uncertainty head (a property of the now-submitted fusion model) is well-ranked on real data and, after the cross-validated post-hoc rescaling above, calibrated to nominal coverage.

6 Conclusion

We presented a staged, honest study of drug-perturbation transcriptome prediction for held-out chemistry on the VCPI DRUG-seq task. A reproducible harness reports the control and mean baselines, a retrieval predictor, a chemistry-foundation fusion decoder, and — as references — a regularized linear model, a deep regressor, and a pretrained chemistry transformer, all under one scaffold split. The central result is a cautionary one about evaluation: the model ranking inverts almost end to end between an inverse-variance proxy and the contest’s true active-set metric. Under the proxy a linear fingerprint baseline appears to win and the deep models look

pointless; under the real metric the deep models win, our fusion decoder significantly beats that linear baseline, and the proxy’s “winner” is the worst chemistry-aware predictor — every gap significant. We submit the fusion decoder, the best of our models on the real metric, and we report the validated scorer (0.535 for the mean baseline, against the organizers’ 0.507). The fusion model’s uncertainty head is well-ranked and post-hoc calibratable, and its chemistry-driven residual decomposes into coherent THP-1 gene programs (stress response, cell cycle, inflammation, hypoxia), so the chemistry signal it recovers is real biology. The transferable lesson is that on real held-out chemistry a benchmark is only as trustworthy as its metric: “simple baselines win” can be an artifact of the score, and which model wins is, here, a property of the metric as much as of the model — a confirmation, on real drug chemistry, of the well-calibrated-metric thesis that Meija et al. [9], Miller et al. [12] establish largely on genetic perturbation.

Acknowledgments

This work was produced at the AIBio Builder Hackathon (Boston Seaport, May 30, 2026), organized by Absentia and partners. We thank the organizers, mentors, and the Ginkgo Bioworks team for hosting the VCPI “Build a Virtual Cell” track and for providing compute credits and feedback.

Data Availability

All training and evaluation data are from the VCPI DRUG-seq dataset, provided by Ginkgo Bioworks, Inc. through the Virtual Cell Prediction Initiative (VCPI, <https://thevirtualcell.com>). The dataset is used here under the terms of the VCPI hackathon. We gratefully acknowledge Ginkgo Bioworks, Inc. as the source of the THP-1 DRUG-seq perturbation data analyzed in this paper.

References

- [1] Constantin Ahlmann-Eltze, Wolfgang Huber, and Simon Anders. 2025. Deep-learning-based gene perturbation effect prediction does not yet outperform simple linear baselines. *Nature Methods* (2025). <https://www.nature.com/articles/s41592-025-02772-6>
- [2] Walid Ahmad, Elana Simon, Seyone Chithrananda, Gabriel Grand, and Bharath Ramsundar. 2022. ChemBERTa-2: Towards Chemical Foundation Models. arXiv:2209.01712. <https://arxiv.org/abs/2209.01712>
- [3] Gerold Csendes, Gema Sanz, Kristóf Z. Szalay, and Bence Szalai. 2025. Benchmarking foundation cell models for post-perturbation RNA-seq prediction. *BMC Genomics* 26:412 (2025). <https://pubmed.ncbi.nlm.nih.gov/40269681/>
- [4] Samuel G. Finlayson, Matthew B. A. McDermott, Alex V. Pickering, Scott L. Lipnick, and Isaac S. Kohane. 2019. Cross-modal representation alignment of molecular structure and perturbation-induced transcriptional profiles. arXiv. <https://arxiv.org/pdf/1911.10241>
- [5] Mahshid Heidari, Mina Karimpour, Sumana Srivatsa, and Hesam Montazeri. 2026. Evaluating Single-Cell Perturbation Response Models Is Far from Straightforward. bioRxiv. <https://www.biorxiv.org/content/10.64898/2026.02.14.705879v1.full>

- [6] Leon Hetzel et al. 2022. Predicting Cellular Responses to Novel Drug Perturbations at a Single-Cell Level (chemCPA). In *NeurIPS*. https://proceedings.neurips.cc/paper_files/paper/2022/file/aa933b5abc1be30baecce1d230ec575a7-Paper-Conference.pdf
- [7] Yiming Li, Min Zeng, Jun Zhu, Linjing Liu, Fang Wang, Longkai Huang, Fan Yang, Min Li, and Jianhua Yao. 2025. Genetic-to-Chemical Perturbation Transfer Learning Through Unified Multimodal Molecular Representations. *bioRxiv*. <https://www.biorxiv.org/content/10.1101/2025.02.02.635055.full.pdf>
- [8] Mohammad Lotfollahi et al. 2023. Predicting cellular responses to complex perturbations in high-throughput screens (CPA). *Molecular Systems Biology* (2023). <https://www.embopress.org/doi/abs/10.15252/msb.202211517>
- [9] Gabriel M. Mejia, Henry E. Miller, Francis J. A. Leblanc, Bo Wang, Brendan Swain, and Lucas Paulo de Lima Camillo. 2025. Diversity by Design: Addressing Mode Collapse Improves scRNA-seq Perturbation Modeling on Well-Calibrated Metrics. *arXiv:2506.22641*. <https://arxiv.org/abs/2506.22641>
- [10] Oscar Méndez-Lucio, Christos Nicolaou, and Berton Earnshaw. 2024. MoIE: a molecular foundation model for drug discovery. *arXiv / Nature Communications*. <https://arxiv.org/pdf/2211.02657>
- [11] Fanbo Meng, Can Wang, Yue Lin, Jing Mo, Xunzhi Zhang, Zhaotong Cong, Chi Song, Sanyin Zhang, Shilin Chen, Liang Leng, and Wei Chen. 2026. DeepICER: A deep learning framework for predicting compound-induced gene expression profiles. *Acta Pharmaceutica Sinica B* (2026). <https://www.sciencedirect.com/science/article/pii/S2211383526001000>
- [12] Henry E. Miller, Gabriel M. Mejia, Francis J. A. Leblanc, Bo Wang, Brendan Swain, and Lucas Paulo de Lima Camillo. 2025. Deep Learning-Based Genetic Perturbation Models Do Outperform Uninformative Baselines on Well-Calibrated Metrics. *bioRxiv* 2025.10.20.683304. <https://www.biorxiv.org/content/10.1101/2025.10.20.683304v1>
- [13] Xiaoning Qi et al. 2024. Predicting transcriptional responses to novel chemical perturbations using a deep generative model for drug discovery (PRnet). *Nature Communications* (2024). <https://www.nature.com/articles/s41467-024-53457-1>
- [14] Eduardo Soares, Victor Shirasuna, Emilio Vital Brazil, Renato Cerqueira, Dmitry Zubarev, and Kristin Schmidt. 2024. A Large Encoder-Decoder Family of Foundation Models for Chemical Language. *arXiv*. <https://arxiv.org/pdf/2407.20267>
- [15] Xiaochu Tong, Ning Qu, Xiangtai Kong, Shengkun Ni, Jingyi Zhou, Kun Wang, Lehan Zhang, Yiming Wen, Jiangshan Shi, Sulin Zhang, Xutong Li, and Mingyue Zheng. 2023. TranSiGen: Deep representation learning of chemical-induced transcriptional profile. *bioRxiv*. <https://www.biorxiv.org/content/10.1101/2023.11.12.566777.full.pdf>
- [16] Augustin Wenteler, Martina Occhetta, Nikhil Branson, Magdalena Huebner, Victor Curean, William T. Dee, William T. Connell, Alex Hawkins-Hooker, Si Pham Chung, Yasha Ektefaie, Aoife Gallagher-Syed, and Charlotte M. V. Córdova. 2024. PertEval-scFM: Benchmarking Single-Cell Foundation Models for Perturbation Effect Prediction. *bioRxiv*. <https://www.biorxiv.org/content/10.1101/2024.10.02.616248.full.pdf>
- [17] Yan Wu, Esther Wershof, Sebastian M. Schmon, Marcel Nassar, Błażej Osiński, Ridvan Eksi, Zichao Yan, Rory Stark, Kun Zhang, and Thore Graepel. 2024. PerturBench: Benchmarking Machine Learning Models for Cellular Perturbation Analysis. *arXiv*. <https://arxiv.org/html/2408.10609v4>
- [18] Chaoyang Ye et al. 2018. DRUG-seq for miniaturized high-throughput transcriptome profiling in drug discovery. *Nature Communications* (2018). <https://pmc.ncbi.nlm.nih.gov/articles/PMC6192987/>
- [19] Linchang Zhu and Yuanhanyu Luo. 2025. DrugPT: A Flexible Framework for Integrating Gene and Chemical Representations in Perturbation Modeling. *bioRxiv*. <https://www.biorxiv.org/content/10.1101/2025.07.25.665130.full.pdf>